

DISCOVERY OF RADIO PULSATIONS FROM THE X-RAY PULSAR J0205+6449 IN SUPERNOVA REMNANT 3C58 WITH THE GREEN BANK TELESCOPE

F. CAMILO,¹ I. H. STAIRS,² D. R. LORIMER,³ D. C. BACKER,⁴ S. M. RANSOM,^{5,6} B. KLEIN,⁷
R. WIELEBINSKI,⁷ M. KRAMER,³ M. A. MCLAUGHLIN,³ Z. ARZOUMANIAN,⁸ AND P. MÜLLER⁷
Accepted for publication in The Astrophysical Journal Letters April 12, 2002

ABSTRACT

We report the discovery with the 100 m Green Bank Telescope of 65 ms radio pulsations from the X-ray pulsar J0205+6449 at the center of supernova remnant 3C58, making this possibly the youngest radio pulsar known. From our observations at frequencies of 820 and 1375 MHz, the free electron column density to PSR J0205+6449 is found to be $140.7 \pm 0.3 \text{ cm}^{-3} \text{ pc}$. The barycentric pulsar period P and \dot{P} determined from a phase-coherent timing solution are consistent with the values previously measured from X-ray observations. The averaged radio profile of PSR J0205+6449 consists of one sharp pulse of width $\approx 3 \text{ ms} \approx 0.05P$. The pulsar is an exceedingly weak radio source, with pulse-averaged flux density in the 1400 MHz band of $\sim 45 \mu\text{Jy}$ and a spectral index of ~ -2.1 . Its radio luminosity of $\sim 0.5 \text{ mJy kpc}^2$ at 1400 MHz is lower than that of $\sim 99\%$ of known pulsars and is the lowest among known young pulsars.

Subject headings: ISM: individual (3C58) — pulsars: individual (PSR J0205+6449) — supernova remnants

1. INTRODUCTION

The “Crab-like” supernova remnant (SNR) G130.7+3.1 (3C58) has long been suspected of containing a pulsar at its center (e.g., Becker, Helfand, & Szymkowiak 1982). This SNR is of particular interest because it is thought to be the remnant of the explosion recorded in 1181 AD (SN 1181), and hence to have a known age of 820 yr. After more than 20 years of searching in the X-ray and radio bands, the pulsar J0205+6449 with period $P = 65.68 \text{ ms}$ was recently discovered at the SNR center with the *Chandra* X-ray Observatory (Murray et al. 2002).

The historical record associating the pulsar-powered synchrotron nebula 3C58 with SN 1181 is compelling. Nevertheless, 3C58 has some properties suggesting a larger age (see, e.g., Slane, Helfand, & Murray 2002, and references therein). Also, the nebular radio emission of 3C58 is $\sim 10\times$ lower than the comparably aged Crab Nebula’s, while the X-ray emission is $\sim 1000\times$ weaker. Because the synchrotron lifetime of X-ray-emitting electrons is short (unlike of those generating radio emission), it is surprising that the ratio of the X-ray luminosities from the 2 SNRs does not match the relative present-day spin-down luminosities of the pulsars: $\dot{E}_{\text{Crab}}/\dot{E}_{\text{J0205+6449}} \approx 15$. Since $\dot{E} \propto \dot{P}/P^3$, the power injected into the nebula as a function of time depends strongly on $P(t)$, which therefore is an important quantity to constrain; the subsequent nebular evolution is governed in addition by the pressure of the ambient medium. The characteristic age $\tau_c = P/2\dot{P} = 5400 \text{ yr}$ of J0205+6449 can be reconciled with the 1181 AD explosion by appealing to a large initial spin period of $\sim 60 \text{ ms}$ (Murray et al. 2002). However we do not know the form of the spin evolution of the pulsar: measuring its “braking index” n , where the angular frequency of rotation evolves as $\dot{\Omega} \propto -\Omega^n$, would constrain $P(t)$ and help

to understand the energetics of 3C58.

The study of J0205+6449 at radio wavelengths could contribute significantly towards the determination of the braking index: precise long-term monitoring of the pulsar rotation, especially important for young pulsars which often experience period glitches, may prove easier from the ground than from satellites. In addition, the absolute phase alignment of radio and X-ray pulses should provide information regarding the emission mechanism. A radio detection would also yield the dispersion measure (DM), giving an independent distance constraint or, alternatively, the average free electron density along the line of sight. Finally, measuring the radio luminosity and spectrum of very young pulsars is essential for constraining the population of these objects in the Galaxy. Motivated by these factors we made deep searches for radio pulsations from PSR J0205+6449, culminating in their discovery with the new Green Bank Telescope as reported here.

2. OBSERVATIONS

The SNR 3C58 was most recently searched for a radio pulsar by Lorimer, Lyne & Camilo (1998), with a resulting flux density limit for the pulsar of $S_{600} < 1.1 \text{ mJy}$ at a search frequency of $\nu = 600 \text{ MHz}$. This corresponds to $S_{1400} < 0.3 \text{ mJy}$ for a median pulsar spectral index of $\alpha = -1.6$ (Lorimer et al. 1995), where $S_\nu \propto \nu^\alpha$. At a distance $d = 3.2 \text{ kpc}$ (Roberts et al. 1993) the implied luminosity limit $L_{1400} \equiv S_{1400}d^2 < 3 \text{ mJy kpc}^2$ is somewhat larger than the radio luminosity of at least one young pulsar (Camilo et al. 2002), and the discovery of X-ray pulsations from PSR J0205+6449 at the center of 3C58 by Murray et al. (2002) led us to attempt more sensitive searches.

On 2001 October 8 we used the 100 m Effelsberg telescope to conduct a search of PSR J0205+6449. We observed the pulsar

¹ Columbia Astrophysics Laboratory, Columbia University, 550 West 120th Street, New York, NY 10027

² National Radio Astronomy Observatory, P.O. Box 2, Green Bank, WV 24944

³ University of Manchester, Jodrell Bank Observatory, Macclesfield, Cheshire, SK11 9DL, UK

⁴ Astronomy Department, University of California, Berkeley, CA 94720

⁵ Physics Department, McGill University, 3600 University Street, Montreal, QC, H3A 2T8, Canada

⁶ Center for Space Research, Massachusetts Institute of Technology, Cambridge, MA 02139

⁷ Max-Planck-Institut für Radioastronomie, Auf dem Hügel 69, D-53121, Bonn, Germany

⁸ Universities Space Research Association/NASA-GSFC, Code 662, Greenbelt, MD 20771

position for 12.5 hr at a center frequency of 1410 MHz. Signals were filtered in 8×4 MHz-wide channels for each of 2 polarizations, after which they were detected and digitized every 0.8 ms. Samples from orthogonal polarizations were added in hardware and the 8 total power time series were written to disk for offline analysis. We also recorded short data sets on strong pulsars for calibration purposes. We analyzed the data in standard fashion (see below for description of the search at Green Bank), de-dispersing the time series for a number of trial DMs in the range 0–500 cm^{-3} pc, with no significant candidates found at the expected period. From these observations we inferred $S_{1400} < 0.1$ mJy for a pulsar duty-cycle of $\sim 0.05P$.

On 2002 February 22–23 we used 18 hr at the Green Bank Telescope to search for radio emission from PSR J0205+6449. We divided the time nearly equally between an observation centered at 1375 MHz with a Gregorian focus receiver, followed by one at 820 MHz with a prime focus receiver. The telescope gain and system temperature, including a large contribution from the SNR, are given in Table 1. We also performed short calibration observations of strong pulsars at both frequencies. The receivers, sampling 2 orthogonal polarizations, had band-limiting filters installed of width 150 and 80 MHz centered on 1375 and 820 MHz respectively. The radio frequency (RF) signals were converted to an intermediate frequency (IF) and transmitted via optical fibers to the control room, where they were passed to the Berkeley-Caltech Pulsar Machine (BCPM).

The BCPM is one of several signal processors of similar design (Backer et al. 1997). The 2 input IF signals are distributed to an array of 2×6 mixer/filter modules. These accept signals from 6 local oscillator modules for baseband mixing and low-pass filtering with the bandwidth set by subsequent signal processing requirements. The signals are sent to 2×6 digital filter boards which 4-bit sample and form detected powers in 16 independent and adjacent frequency channels. The BCPM is thus an analog/digital filter bank with 2×96 channels. Time decimation of the power samples and optional summing of the 2 IFs (which we used) is accomplished in combiner boards. The combiner board output is reduced to 4-bit power deviation by mean removal and scaling. The power vector(s) are passed to the host Sun workstation through an EDT⁹ DMA card. The Sun attaches a header and places data on a disk for offline processing as well as monitoring data quality¹⁰. For our 2 observations we used the data-taking parameters listed in Table 1.

3. DATA ANALYSIS AND RESULTS

Although we knew the pulsar period a priori, we did not know its DM and chose to use standard search algorithms to analyze the data. Also, despite the presence of strong RF interference (RFI) visible in a spectrum analyzer during data collection (most notably as persistent radar in the 1400 MHz band and sporadic but very strong RFI of unknown origin in the 800 MHz band) in a first pass we masked no portions of the fluctuation spectra. For both observations data from 2^{25} decimated time samples (see Table 1) were de-dispersed at 204 trial DMs in the range 0–203 cm^{-3} pc (the DM predicted by the Taylor & Cordes 1993 electron density/distance model is ~ 70 cm^{-3} pc). Each of the 204 resulting time series was then searched for periodic signals over a range of duty cycles with an FFT-based code (described in detail by Lorimer et al. 2000) identifying signif-

icant features in the fundamental amplitude spectrum as well as in spectra with 2, 4, 8, and 16 harmonics folded in. The 1375 MHz data were heavily corrupted by RFI — in particular the 182nd harmonic of a radar signal repeating every ~ 12 s coincided with the expected pulsar rotation frequency. Therefore we eventually reanalyzed these data while blanking the radar frequency and its first 150 harmonics in the amplitude spectra.

The 820 MHz data were clean in the spectral range of interest and a signal was unambiguously detected at the expected period and clearly dispersed, peaking at $\text{DM} \approx 143$ cm^{-3} pc with a signal-to-noise ratio $S/N = 10.9$, as shown in Figure 1. After excision of the radar-related RFI, the 1375 MHz data yielded a signal at the same period within the uncertainty peaking at $\text{DM} \approx 140$ cm^{-3} pc with $S/N = 8.8$.

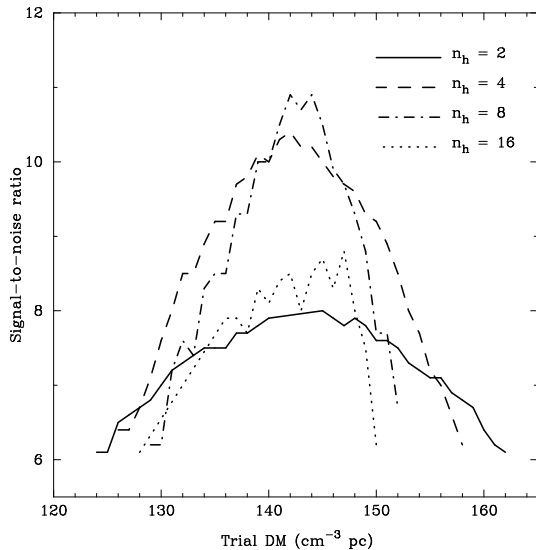


FIG. 1.— Search signal-to-noise ratio as a function of trial dispersion measure (DM) for the candidate with period $P \approx 65.69$ ms in the 820 MHz data set. Each curve corresponds to the addition of the number of harmonics indicated.

We then measured pulse times-of-arrival (TOAs) referenced to the observatory atomic time standard from both data sets: 6 good TOAs were obtained in each of the 800 and 1400 MHz bands with individual uncertainty ≈ 0.5 ms. A further 17 TOAs of similar quality were obtained on 8 additional days of observations, with a total data span of 35 d. We used the TOAs and the TEMPO timing software¹¹ to fit for P , \dot{P} , and DM, obtaining the values listed in Table 2. The table also lists the celestial coordinates of PSR J0205+6449 obtained by Slane et al. (2002), which were held fixed in our timing fit. Our values of P and \dot{P} determined from a phase-connected timing solution spanning 35 d are much more precise than, but agree with, the equivalent values obtained by Murray et al. (2002) based on only 2 periods measured 1.2 and 4.4 yr before: the barycentric period P listed in Table 2 differs by 15 ± 18 ns from that extrapolated to the epoch of our observations using the P and \dot{P} determined by Murray et al., while our \dot{P} is consistent with theirs at the 2σ level. Such a close match of spin parameters over an interval greater than 4 yr suggests that no significant period glitch occurred during this time span.

Both search data sets, de-dispersed at $\text{DM} = 141$ cm^{-3} pc and folded at the best search periods, are shown in Figure 2. The average pulse profile at both frequencies consists of a single

⁹ Engineering Design Team, Inc.

¹⁰ For further details of BCPM installation at Green Bank see <http://www.gb.nrao.edu/~dbacker>.

¹¹ See <http://pulsar.princeton.edu/tempo>.

narrow pulse of width $\approx 0.05P$ (see Table 2); such a profile is expected based on Figure 1, where the search S/N is a maximum for 8 harmonics summed. There is no evidence for the existence of an interpulse at either frequency with amplitude $\gtrsim 15\%$ that of the sharp pulse, in contrast with the X-ray profiles that show an interpulse with amplitude $\sim 30\%$ that of the main pulse (Murray et al. 2002).

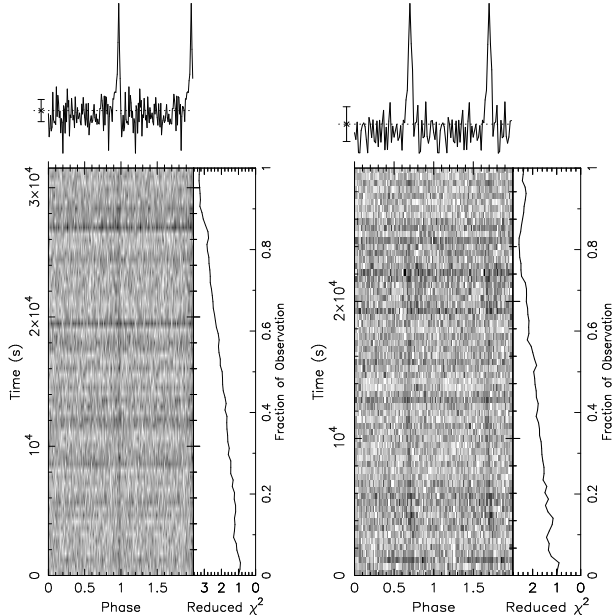


FIG. 2.— Pulse profiles of PSR J0205+6449 displayed as a function of time (bottom) and summed (top). *Left*: Data at a center frequency of $\nu = 1375$ MHz presented with 100 phase bins. The pulse full-width at half maximum (FWHM) is 2.3 ± 0.3 ms. *Right*: Data at $\nu = 820$ MHz displayed with 60 bins. The pulse FWHM is 3.8 ± 0.4 ms. All data were de-dispersed at $DM = 141 \text{ cm}^{-3} \text{ pc}$ and one phase bin in each panel matches the dispersion smearing resolution of the respective profile. Two full periods are shown at each frequency for clarity. The increasing/decreasing slope of each reduced χ^2 curve traces pulsation significance as measured against a constant flux (or non-pulsed) model. Decreases in reduced χ^2 are most likely caused by interstellar scintillation or RFI.

Note that the S/N in the 820 MHz data appears to be smaller near the beginning of the integration and again towards the end (Fig. 2), possibly as a consequence of scintillation. Assuming that the search S/Ns in the 2 long integrations reflect the respective long-term time-averaged flux densities in both frequency bands, we have integrated the area under the pulse profiles and measured their baseline rms to determine the respective flux densities. We converted to a Jy scale using the observing parameters listed in Table 1 together with the radiometer equation (Dicke 1946). In this manner we estimate that $S_{1400} \sim 45 \mu\text{Jy}$ and $S_{800} \sim 130 \mu\text{Jy}$, with $\sim 25\%$ accuracy. The resulting spectral index in the 800–1400 MHz range is $\alpha \sim -2.1 \pm 0.6$, and the radio luminosity is $L_{1400} \sim 0.5 (d/3.2 \text{ kpc})^2 \text{ mJy kpc}^2$. These values will be much improved by the averaging of several calibrated observations.

The 947 yr-old Crab pulsar was detected initially through its individual “giant” pulses rather than through its time-averaged pulsed emission (Staelin & Reifenstein 1968). As the emission of giant pulses may be related to the magnetic field strength at the pulsar light cylinder, B_{lc} (e.g., Cognard et al. 1996), and PSR J0205+6449 has the 10th largest value of B_{lc} among known pulsars, we searched for aperiodic, dispersed pulses from PSR J0205+6449. No excess of single pulses was found

at the DM of the pulsar. Inferring a quantitative limit is complicated by significant levels of RFI, and this search will be reported in detail elsewhere.

4. DISCUSSION

We have discovered radio pulsations from the direction of PSR J0205+6449 in SNR 3C58 in an unbiased search of 2 independent data sets acquired at center frequencies of 820 and 1375 MHz. The pulsations are clearly dispersed and have a precisely determined period matching that observed from PSR J0205+6449 at X-ray wavelengths (Murray et al. 2002). We have therefore discovered radio pulsations that are unambiguously from PSR J0205+6449 which supplants the Crab pulsar as the youngest neutron star with known radio emission.

The $DM = 141 \text{ cm}^{-3} \text{ pc}$ of PSR J0205+6449, located at $(l, b) = (130^\circ 72, 3^\circ 08)$, is approximately twice that predicted by the Taylor & Cordes (1993) model for the usually accepted distance to 3C58 (3.2 kpc, determined from H I absorption measurements¹²). This implies an average free electron density to 3C58 of $n_e \approx 0.044 \text{ cm}^{-3}$. The neutral column density to the SNR is $3 \times 10^{21} \text{ cm}^{-2}$ (Helfand, Becker, & White 1995), implying an ionized fraction of roughly 15%, which is somewhat higher than might be expected towards the Galactic plane. However, the SNR lies on the eastern edge of the large W3/W4/W5 complex of H II regions (e.g., Reynolds, Sterling, & Haffner 2001), and in fact may be on the edge of a cavity being ionized by the star-forming regions (R. J. Reynolds and G. Madsen, private communication). It is not known if the progenitor of SN 1181 belonged to, or was a runaway star from, this region of star formation. In any case, the relative locations of 3C58 and W3/W4/W5 may account for the apparent excess of ionized material towards the pulsar.

We note that the reported detection of PSR J0205+6449 with $DM = 24 \text{ cm}^{-3} \text{ pc}$ at a frequency of 110 MHz (Malofeev, Malov, & Glushak 2001) is incompatible with the results we present: the dispersion smearing timescale for a signal with $DM = 141 \text{ cm}^{-3} \text{ pc}$ within one of the 20 kHz-wide spectral channels used by Malofeev et al. (2001) at 110 MHz is 17 ms. De-dispersing and summing their 32 individual such channels with $DM = 24 \text{ cm}^{-3} \text{ pc}$ would result in an overall smearing of the pulse far in excess of $P = 65$ ms, rendering pulsations unobservable from PSR J0205+6449.

The main X-ray pulse from PSR J0205+6449 has essentially the same sharp structure and width ($\approx 0.04P$; Murray et al. 2002) as the radio pulse (Fig. 2 and Table 2). This morphology suggests that the X-ray emission is likely magnetospheric in nature, but absolute alignment of radio and X-ray profiles will provide further clues for understanding the emission mechanism(s). Considering the obvious existence of magnetospheric emission, we might expect this pulsar to be a γ -ray source. The flux sensitivity of the EGRET instrument to emission from PSR J0205+6449, using a photon index $\Gamma = 2$ typical of γ -ray-emitting pulsars, is $F_\gamma \sim 5 \times 10^{32} \text{ erg s}^{-1} \text{ kpc}^{-2}$ ($> 100 \text{ MeV}$; Hartman et al. 1999), corresponding to a luminosity limit $L_\gamma \equiv F_\gamma d^2 \lesssim 5 \times 10^{33} \text{ erg s}^{-1}$. With spin-down luminosity $\dot{E} = 2.7 \times 10^{37} \text{ erg s}^{-1}$, its efficiency at converting rotational power into beamed high-energy γ -rays is $\eta \equiv L_\gamma / \dot{E} \lesssim 2 \times 10^{-4}$. This compares to $\eta \sim 10^{-4}$ for the Crab pulsar, with the largest value of \dot{E} known in the Galaxy, and larger efficiencies for

¹² Depending on data set and Galactic rotation curve used, the inferred distance ranges from 2.6 kpc to “just beyond” 3.2 kpc (see Roberts et al. 1993, and references therein). We adopt $d = 3.2 \text{ kpc}$ in this Letter.

(generally older) pulsars with smaller values of \dot{E} such as Vela ($\eta \sim 6 \times 10^{-4}$) and Geminga ($\eta \sim 0.02$). If PSR J0205+6449 follows the approximate $\eta \propto E^{-1/2}$ relation that seems to apply to known γ -ray-emitting pulsars (Thompson et al. 1999), its flux may be just below the detection threshold of EGRET and should be detected by next-generation observatories such as *GLAST*.

The discovery of extremely weak radio pulsations from PSR J0205+6449 highlights the vexing issue of the true luminosity distribution of (particularly young) pulsars. The past year has witnessed the discovery of 3 very young ($\tau_c \lesssim 10$ kyr) radio-emitting pulsars with $0.5 \lesssim L_{1400} \lesssim 3$ mJy kpc², 1–2 orders of magnitude less luminous than any young pulsars previously known (Halpern et al. 2001; Camilo et al. 2002, this Letter). It now seems abundantly clear that we have yet to probe the depths of the luminosity function of young pulsars. The state-of-the-art for finding young radio pulsars (~ 10 hr integrations at telescopes with gain $\gtrsim 1$ K Jy⁻¹ and bandwidths 100–300 MHz at $\nu \sim 1400$ MHz) yields limits usually no better than $L_{1400} \sim 1$ mJy kpc². Nevertheless, many worthy targets remain to be searched at this level. Improving the existing limits helps to constrain better the “beaming fraction” for young pulsars (e.g., Frail & Moffett 1993, based in part on the non-detection of the pulsar in 3C58 with a limit of 0.15 mJy at 1400 MHz,

estimated a beaming fraction of 0.6 which needs to be revised in light of recent discoveries), and is important for building an accurate census of Galactic neutron stars. In this regard, the detection of PSR J0205+6449, an 820 yr-old pulsar, at a frequency of 820 MHz — only the 2nd pulsar ever discovered in the 800 MHz band (D’Amico et al. 1988) — suggests that the availability of the magnificent GBT provides a new region of phase space with significant, and as yet untapped, discovery potential.

We are deeply grateful to the dedicated staff of NRAO, and in particular to the GBT project team, whose hard work has made the Robert C. Byrd Green Bank Telescope a great research instrument. We thank Bryan Jacoby and Stuart Anderson for assistance with the BCPM, Jay Lockman for helpful discussions, and David Helfand for early communication of discovery of X-ray pulsations. The National Radio Astronomy Observatory is a facility of the National Science Foundation operated under cooperative agreement by Associated Universities, Inc. FC acknowledges support from NASA grants NAG 5-9095 and NAG 5-9950. IHS is a Jansky Fellow. DRL is a University Research Fellow funded by the Royal Society. SMR is a McGill University Tomlinson Fellow.

REFERENCES

- Backer, D. C., Dexter, M. R., Zepka, A., Ng, D., Werthimer, D. J., Ray, P. S., & Foster, R. S. 1997, *PASP*, 109, 61
 Becker, R. H., Helfand, D. J., & Szymkowiak, A. E. 1982, *ApJ*, 255, 557
 Camilo, F., Manchester, R. N., Gaensler, B. M., Lorimer, D. R., & Sarkissian, J. 2002, *ApJ*, 567, L71
 Cognard, I., Shrauner, J. A., Taylor, J. H., & Thorsett, S. E. 1996, *ApJ*, 457, L81
 D’Amico, N., Manchester, R. N., Durdin, J. M., Stokes, G. H., Stinebring, D. R., Taylor, J. H., & Brissenden, R. J. V. 1988, *MNRAS*, 234, 437
 Dicke, R. H. 1946, *Rev. Sci. Instrum.*, 17, 268
 Frail, D. A. & Moffett, D. A. 1993, *ApJ*, 408, 637
 Halpern, J. P., Camilo, F., Gotthelf, E. V., Helfand, D. J., Kramer, M., Lyne, A. G., Leighly, K. M., & Eracleous, M. 2001, *ApJ*, 552, L125
 Hartman, R. C. et al. 1999, *ApJS*, 123, 79
 Helfand, D. J., Becker, R. H., & White, R. L. 1995, *ApJ*, 453, 741
 Lorimer, D. R., Kramer, M., Müller, P., Wex, N., Jessner, A., Lange, C., & Wielebinski, R. 2000, *A&A*, 358, 169
 Lorimer, D. R., Lyne, A. G., & Camilo, F. 1998, *A&A*, 331, 1002
 Lorimer, D. R., Yates, J. A., Lyne, A. G., & Gould, D. M. 1995, *MNRAS*, 273, 411
 Malofeev, V., Malov, O., & Glushak, A. 2001. IAU circular 7775
 Murray, S. S., Slane, P. O., Seward, F. D., Ransom, S. M., & Gaensler, B. M. 2002, *ApJ*, 568, 226
 Reynolds, R. J., Sterling, N. C., & Haffner, L. M. 2001, *ApJ*, 558, L101
 Roberts, D. A., Goss, W. M., Kalberla, P. M., Herbstmeier, U., & Schwarz, U. J. 1993, *A&A*, 274, 427
 Slane, P. O., Helfand, D. J., & Murray, S. S. 2002, *ApJ*, in press (*astro-ph/0204151*)
 Staelin, D. H. & Reifenstein, III, E. C. 1968, *Science*, 162, 1481
 Taylor, J. H. & Cordes, J. M. 1993, *ApJ*, 411, 674
 Thompson, D. J. et al. 1999, *ApJ*, 516, 297

TABLE 1
SUMMARY OF OBSERVATIONS AND ANALYSES AT GBT

Observing frequency (MHz)	1375	820
Telescope gain (K Jy^{-1})	2.0	2.0
System temperature on cold sky (K) . . .	20	25
Galactic synchrotron temperature (K) . .	2	9
SNR 3C58 temperature (K)	64	67
Spectral channel width (MHz)	1.4	0.5
Sample time (μs)	50	72
Integration time (hr)	8.75	8.25
Effective time resolution of search (ms)	0.9	0.864
Effective integration time of search (hr)	8.4	8.1

TABLE 2
PARAMETERS OF PSR J0205+6449

Parameter	Value
R.A. (J2000) ^a	02 ^h 05 ^m 37 ^s .92
Decl. (J2000) ^a	+64°49'42".8
Period, P (ms)	65.68638162(2)
Period derivative, \dot{P}	$1.9393(4) \times 10^{-13}$
Epoch (MJD [TDB])	52345.0
Dispersion measure, DM ($\text{cm}^{-3} \text{pc}$) . . .	140.7(3)
Pulse FWHM at 1375 MHz (ms)	2.3 ± 0.3
Pulse FWHM at 820 MHz (ms)	3.8 ± 0.4
Flux density at 1375 MHz, S_{1400} (μJy)	~ 45
Flux density at 820 MHz, S_{800} (μJy) . .	~ 130
Distance of SNR 3C58, d (kpc)	≈ 3.2
Derived parameters:	
Radio luminosity, L_{1400} (mJy kpc^2) . .	~ 0.5
Spectral index, α	$\sim -2.1 \pm 0.6$
Mean free electron density, n_e (cm^{-3})	≈ 0.044

Note. — Numbers in parentheses represent 1σ uncertainties in the least-significant digits of fitted parameters.

^aPosition known with $\approx 0''.5$ accuracy from *Chandra* data (Slane et al. 2002).